environmental microbiology reports

Environmental Microbiology Reports (2014) **6**(5), 448–458 doi:10.1111/1758-2229.12147

Effects of engineered silver nanoparticles on the growth and activity of ecologically important microbes

Jessica Beddow,[1] Björn Stolpe,[2] Paula Cole,[2] Jamie R. Lead,[2†] Melanie Sapp,[3] Brett P. Lyons,[4] Ian Colbeck[1] and Corinne Whitby[1*]

[1]*School of Biological Sciences, University of Essex, Essex, CO4 3SQ, UK.*

[2]*School of Geography, Earth and Environmental Sciences, University of Birmingham, Birmingham, UK.*

[3]*Food and Environment Research Agency, Sand Hutton, York, UK.*

[4]*Centre for Environment, Fisheries and Aquaculture Science, Weymouth, Dorset, UK.*

Summary

Currently, little is known about the impact of silver nanoparticles (AgNPs) on ecologically important microorganisms such as ammonia-oxidizing bacteria (AOB). We performed a multi-analytical approach to demonstrate the effects of uncapped nanosilver (uAgNP), capped nanosilver (cAgNP) and Ag_2SO_4 on the activities of the AOB: *Nitrosomonas europaea*, *Nitrosospira multiformis* and *Nitrosococcus oceani*, and the growth of *Escherichia coli* and *Bacillus subtilis* as model bacterial systems in relation to AgNP type and concentration. All Ag treatments caused significant inhibition to the nitrification potential rates (NPRs) of *Nitrosomonas europaea* (decreased from 34 to < 16.7 μM NH_4^+ oxidized day^{-1}), *Nitrosospira multiformis* (decreased from 46 to < 24.8 μM NH_4^+ oxidized day^{-1}) and *Nitrosococcus oceani* (decreased from 26 to < 18.4 μM NH_4^+ oxidized day^{-1}). *Escherichia coli*-Ag interactions revealed that the percentage of damaged *E. coli* cells was 45% greater with Ag_2SO_4, 39% with cAgNPs and 33% with uAgNPs compared with controls. Generally, the inhibitory effect on AOB NPRs and *E. coli*/*B. subtilis* growth was in the following order Ag_2SO_4 > cAgNP > uAgNP. In conclusion, AgNPs (especially cAgNPs) and Ag_2SO_4 adversely affected AOB activities and thus have the potential to severely impact key microbially driven processes such as nitrification in the environment.

Received 20 December, 2013; accepted 22 December, 2013. *For correspondence. E-mail cwhitby@essex.ac.uk; Tel. +44 (01206) 872062; Fax +44 (01206) 872592. †Present address: Center for Environmental Nanoscience and Risk, University of South Carolina, Columbia, SC 29028, USA.

Introduction

Engineered silver nanoparticles (AgNPs) are increasingly being used as a broad spectrum antimicrobial agent in a number of consumer products including medical equipment, clothing, pharmaceuticals, food storage containers, children's toys, cosmetics, optical devices and household appliances (Kim *et al.*, 2007; PEN, 2013). However, AgNPs are readily released from these products during use, and so it is inevitable that they will enter the environment, with potential implications for key microbially driven processes (Moore, 2006; Nowack and Bucheli, 2007; Klaine *et al.*, 2008). When AgNPs are released into natural systems, the chemical and physical properties of the nanoparticles may be transformed by biotic and abiotic processes, which in turn will influence their antibacterial activities. The presence of stabilizing or capping agents may influence the types of transformation that occur, for example, aggregation behaviour and dissolution rate (Tejamaya *et al.*, 2012). In order to accurately assess the environmental risks of AgNPs, a better understanding of the effects of AgNP type and concentration on key functional groups of microorganisms is required. Despite this, knowledge of AgNPs in relation to ecologically important microorganisms is limited.

Nitrification is crucial in the global cycling of nitrogen and is a key step in the removal of nitrogen from environments such as wastewater treatment facilities (Prosser, 1989; Kowalchuck and Stephen, 2001). Ammonia-oxidation is the first and rate-limiting step of nitrification and is mediated by ammonia-oxidizing bacteria (AOB) and ammonia-oxidizing archaea (Prosser and Nicol, 2008). AOB are notoriously sensitive microorganisms, whose activity and viability are susceptible to changes in pH, temperature, salinity, light, dissolved oxygen and sulphide concentration (Joye and Hollibaugh, 1995; Strauss and Dodds, 1997; Rysgaard *et al.*, 1999; Nicol *et al.*, 2008). It is therefore not unreasonable to predict that AgNPs entering terrestrial and aquatic ecosystems (such as via wastewater treatment facilities) may disrupt ammonia oxidizers and hence nitrification rates.

The present study focused on two different types of AgNPs: uncapped (uAgNPs) and capped (cAgNPs),

using different model bacterial systems to evaluate the environmental impact of such AgNPs on ammonia oxidizers, a key functional group of microorganisms involved in nitrification. We focused on methoxy-polyethylene-*glycol* (mPEG), a capping agent, which is commonly used to stabilize AgNPs and aid dispersion (Christian *et al*., 2008). Specifically, the study investigated the effect of different concentrations (0.5–50 mg l^{-1}) of uAgNPs, cAgNPs and Ag_2SO_4 on nitrification potential rates (NPRs) using three different AOB species: *Nitrosomonas europaea*, *Nitrosospira multiformis* and *Nitrosococcus oceani*. The AgNP concentrations were selected based on the potential future environmental concentrations or concentrations that would arise in the event of an incidental spill (Gottschalk *et al*., 2009). The effects of uAgNPs, cAgNPs and Ag_2SO_4 on the growth and viability of *Escherichia coli* and *Bacillus subtilis* were also examined. The overall goal of the study was to use a multi-analytical approach and different model bacterial systems, to demonstrate the potential impacts of engineered AgNPs on a key functional group of microorganisms, important in nitrification in the environment.

Results and discussion

Characterization of uAgNPs and cAgNPs

The uAgNPs and cAgNPs were characterized in terms of their morphologies and size distribution (Table 1). The average diameter of the uAgNPs was found to be 118–188 nm, which was up to fivefold larger than the cAgNPs (average diameter 17–40 nm). Transmission electron microscopy (TEM) micrographs showed that the cAgNPs were predominantly present as single particles, while the uAgNPs tended to form aggregates (Fig. 1). Atomic force microscopy confirmed the cAgNPs were predominantly present as single particles (Supporting Information Fig. S1). Asymmetrical flow field flow fractionation confirmed that the cAgNPs had a smaller size distribution compared to the uAgNPs (Supporting Information Fig. S2). The data show that the average AgNP diameters varied depending on the technique used. This is not uncommon in nanoparticle studies and demonstrates the importance of using a multimethod approach for nanoparticle characterization (Domingos *et al*., 2009; MacCuspie *et al*., 2011; Baalousha and Lead, 2012).

The ζ (zeta)-potential and aggregation behaviour of uAgNPs were both strongly influenced by the medium the uAgNPs were dispersed in. Specifically, the ζ-potential increased by almost twofold (from −32 to −17 mV) in Luria–Burtani (LB) broth compared with ultra-high purity (UHP) water (Table 1). In addition, the zeta average hydrodynamic diameter (measured by dynamic light scattering) increased by over twofold (from 188 to 495 nm) in LB broth compared with UHP water (Table 1). In contrast with the uAgNPs, the hydrodynamic diameter of the cAgNPs was unaffected in LB broth (35 nm) (Table 1). Dialysis measurements were performed to determine the rate of Ag^+ dissolution from AgNPs and Ag_2SO_4. Results showed that there were no differences in the rate of Ag^+ dissolution between the cAgNPs and uAgNPs measured over 51 h (i.e. encompassing the time the bacteria were exposed to AgNPs) (Supporting Information Fig. S3). However, the Ag_2SO_4 dissolution was generally greater than the nanoparticle dissolution over 51 h (Supporting Information Fig. S3).

Table 1. Characteristics of uAgNPs and cAgNPs in UHP water and LB broth.

Nanoparticle type	uAgNPs		cAgNPs	
Medium Characteristic (unit) (method)	UHP water	LB broth	UHP water	LB broth
Zeta potential (mV) and pH (DLS)[a]	−32 (± 0.2) (pH7.2)	−17 (± 0.6) (pH 7.2)	−37 (± 0.3) (pH8.1)	−6 (± 0.5) (pH 7.2)
Zeta average hydrodynamic diameter (nm) (DLS)[a]	188 (± 24)	495 (± 48)	35 (± 0.2)	35 (± 0.6)
Number-average hydrodynamic diameter (nm) (FIFFF)[b]	135	ND	31 (± 0.4)	ND
Weighted-average hydrodynamic diameter (nm) (FIFFF)[b]	157	ND	40 (± 1.1)	ND
Average diameter (nm) (TEM)[c]	118 (± 11)	ND	27 (± 1)	ND
Average hydrodynamic diameter (nm) (AFM)[d]	ND	ND	17 (± 10)	ND
Surface area (m^2 g^{-1}) (BET)[e]	2.2 (± 0.1)	ND	ND	ND
Surface area (m^2 g^{-1}) calculated from TEM average diameter	4.9 (± 0.6)	ND	21.2 (± 0.1)	ND

a. Zeta potential and Z-average diameter measurements are reported as the mean of triplicate runs, with five measurements made in each run.
b. FIFFF was carried out on a single uAgNP sample and triplicate cAgNP samples.
c. The diameters of at least 100 cAgNPs and uAgNPs were determined from a minimum of three TEM micrographs.
d. The heights of 67 cAgNPs were determined from a minimum of five AFM micrographs.
e. The mean data for triplicate runs is presented.
Numbers given in brackets represent the standard error of the mean.
AFM, atomic force microscopy; BET, Brunauer, Emmett and Teller theory; DLS, dynamic light scattering; FIFFF, flow field flow fractionation; ND, not determined.

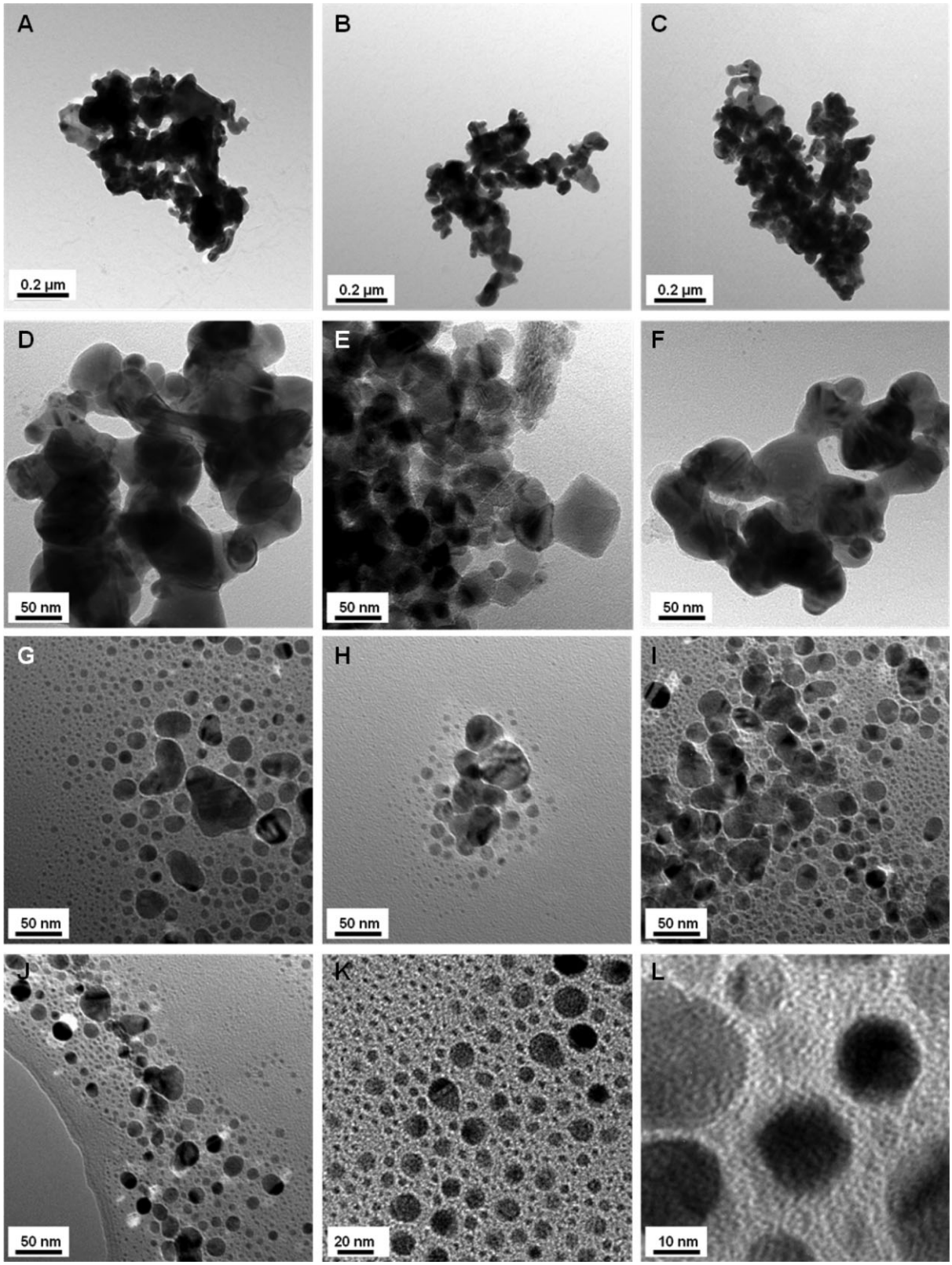

Fig. 1. Representative TEM micrographs of uAgNPs (A–F) and cAgNPs (G–L).

Effect of AgNPs and Ag_2SO_4 on AOB NPRs

Nitrification, driven by ammonia oxidizers, is an important process in global nitrogen cycling. Herein, the effect of uAgNPs, cAgNPs and Ag_2SO_4 was investigated using pure cultures of AOB. It was notable that NPR inhibition varied depending on AOB species, AgNP type and AgNP concentration. All Ag treatments (uAgNPs, cAgNPs and Ag_2SO_4) significantly inhibited the NPRs of *Nitrosomonas europaea* ($F_{18,56} = 153.7$, $P < 0.01$), *Nitrosospira multiformis* ($F_{18,56} = 177.6$, $P < 0.01$) and *Nitrosococcus oceani* ($F_{18,56} = 50.0$, $P < 0.01$) (Fig. 2). In general, the inhibitory effect on AOB NPRs was in the following order: Ag_2SO_4 > cAgNP > uAgNP. Specifically, complete, or almost-complete, inhibition of *Nitrosomonas europaea* and *Nitrosospira multiformis* NPRs occurred when cells were incubated with Ag_2SO_4 between 0.5 and 50 mg l^{-1} ($P < 0.01$) (Fig. 2). While *Nitrosococcus oceani* NPRs were unaffected by 0.5 mg l^{-1} concentrations of Ag_2SO_4, at 5–50 mg l^{-1} Ag_2SO_4 almost-complete inhibition to NPRs occurred ($P < 0.01$) (Fig. 2).

When *Nitrosomonas europaea* and *Nitrosospira multiformis* were incubated with cAgNPs (at 0.5–50 mg l^{-1}), NPRs were significantly inhibited (between 3.2 and 24.8 μM NH_4^+ oxidized day^{-1}; $P < 0.01$) compared with controls without AgNPs (<46 μM NH_4^+ oxidized day^{-1}) (Fig. 2). Interestingly, for *Nitrosospira multiformis*, NPR inhibition by 5 mg l^{-1} of cAgNPs was significantly less than that at 0.5 mg l^{-1} ($P < 0.01$). Also for *Nitrosomonas europaea*, NPR inhibition by 50 mg l^{-1} of cAgNPs was significantly less than that at 5 mg l^{-1} ($P < 0.01$) (Fig. 2). While 0.5 mg l^{-1} of cAgNPs did not affect *Nitrosococcus oceani* NPRs, cAgNPs (at 5–50 mg l^{-1}) significantly inhibited NPRs (between 2.8 and 18.4 μM NH_4^+ oxidized day^{-1}; $P < 0.05$) compared with controls (26 μM NH_4^+ oxidized day^{-1}) (Fig. 1). The observed increase in NPRs from *Nitrosomonas europaea* and *Nitrosospira multiformis* grown with increasing concentrations of cAgNPs may be due to a dose-dependent effect on the behaviour of the nanoparticles (i.e. greater concentrations of nanoparticles lead to a greater likelihood of nanoparticle aggregation, which may result in reduced nanoparticle-AOB cell contact).

Nitrosomonas europaea NPRs were significantly inhibited with uAgNPs at 0.5–50 mg l^{-1} (3.1–6.3 μM NH_4^+ oxidized day^{-1}; $P < 0.01$) compared with controls (34 μM NH_4^+ oxidized day^{-1}) (Fig. 2). While *Nitrosospira multiformis* NPRs were unaffected by 0.5 mg l^{-1} of uAgNPs, 5 and 50 mg l^{-1} significantly inhibited NPRs (between 3.0 and 3.8 μM NH_4^+ oxidized day^{-1}; $P < 0.01$) compared with controls (46 μM NH_4^+ oxidized day^{-1}) (Fig. 2). *Nitrosococcus oceani* NPRs were significantly inhibited with 50 mg l^{-1} uAgNPs (2.8 μM NH_4^+ oxidized day^{-1}; $P < 0.01$) compared with controls (26 μM NH_4 oxidized day^{-1}) (Fig. 2). Specifically, *Nitrosomonas europaea* NPRs were more severely affected by 0.5 mg l^{-1} uAgNPs than *Nitrosospira multiformis* which may be a result of physiological differences between bacterial species. Such findings have implications towards nitrification in wastewater treatment facilities where *Nitrosomonas europaea* are commonly found to dominate (Siripong and Rittmann, 2007).

Differences observed in NPR inhibition are also likely to be associated with the behaviour and aggregation state of the nanoparticles in the different growth media used. For example, *Nitrosomonas europaea* and *Nitrosospira multiformis* were grown in freshwater medium, whereas *Nitrosococcus oceani* was grown in seawater medium. It is likely that the greater ionic strength (3.5%) of the seawater medium caused the cAgNPs and uAgNPs to aggregate, resulting in the observed reduced inhibition by uAgNPs and cAgNPs of *Nitrosococcus oceani* NPRs (Christian *et al*., 2008; Handy *et al*., 2008b).

When *Nitrosomonas europaea* cells were exposed to mPEG (at equivalent concentrations found in 0.5–50 mg l^{-1} cAgNP), NPRs were significantly inhibited (between 2.5 and 23.7 μM NH_4^+ oxidized day^{-1}; $P < 0.01$) compared with controls (34 μM NH_4^+ oxidized day^{-1}) (Fig. 2). In addition, *Nitrosospira multiformis* NPRs were significantly inhibited when cells were exposed to mPEG, at equivalent concentrations found in 50 mg l^{-1} cAgNP (19.8 μM NH_4^+ oxidized day^{-1}; $P < 0.01$), compared with controls (46 μM NH_4^+ oxidized day^{-1}) (Fig. 2). It is possible that capping agents may also contribute towards nanoparticle toxicity (Handy *et al*., 2008b). In the present study, the mPEG capping agent did adversely affect the NPRs of *Nitrosomonas europaea* and (to a lesser extent) *Nitrosospira multiformis*. The exact mechanisms of mPEG toxicity to these AOB are not clear; however, we postulate that the mPEG may interact with the active site of ammonia monoxygenase (AMO), as it has been shown previously that organic compounds may directly bind to the copper atoms in the active site of AMO, inhibiting AMO catalytic ability (Bedard and Knowles, 1989).

Bacterial growth and viability when exposed to AgNPs and Ag_2SO_4

The potential antibacterial activity of uAgNPs, cAgNPs and Ag_2SO_4 was investigated using *E. coli* and *B. subtilis* (Fig. 3). Ag_2SO_4 caused the greatest inhibition of growth in both *E. coli* and *B. subtilis*, followed by cAgNPs and uAgNPs (Fig. 3). Although uAgNPs at 0.5 and 5 mg l^{-1} caused no significant difference in *E. coli* cell growth compared with controls, uAgNPs at 50 mg l^{-1} resulted in a significant reduction in cell density (1.1×10^6 cells ml^{-1}; $P < 0.05$) by 12 h compared with controls (5.1×10^6 cells ml^{-1}) (Fig. 3A). With 0.5 mg l^{-1} cAgNPs, *E. coli* cell

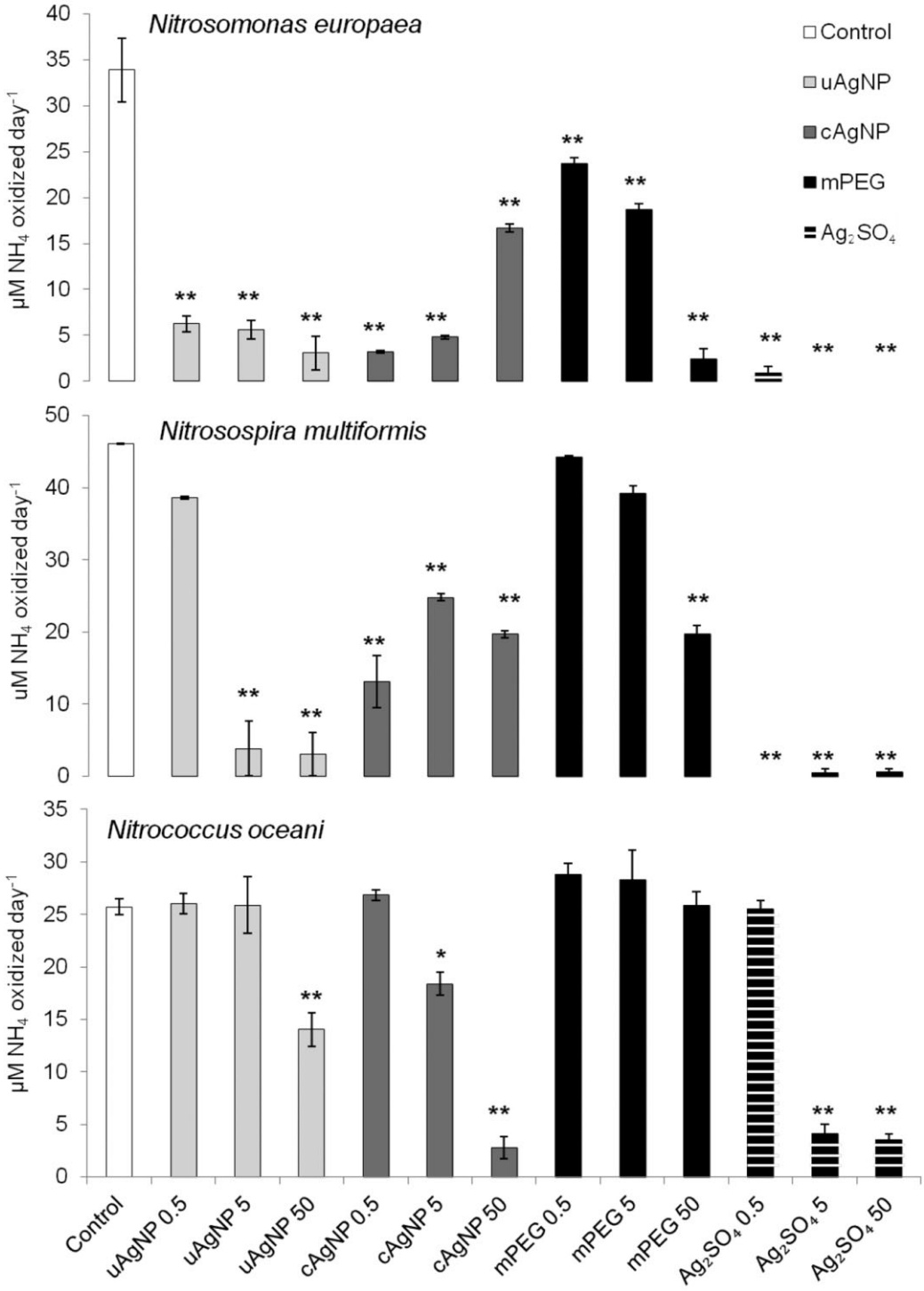

Fig. 2. NPRs of *Nitrosomonas europaea*, *Nitrosospira multiformis* and *Nitrosococcus oceani* in the presence of uAgNPs, cAgNPs, mPEG and Ag_2SO_4 at different concentrations. Significant results are shown by * ($P \leq 0.05$) and ** ($P \leq 0.01$). Error bars represent the standard error of the mean ($n = 3$). White bars represent no-nanoparticle controls, coloured bars represent exposure to uAgNPs (light grey), cAgNPs (dark grey), mPEG (black) and Ag_2SO_4 (striped).

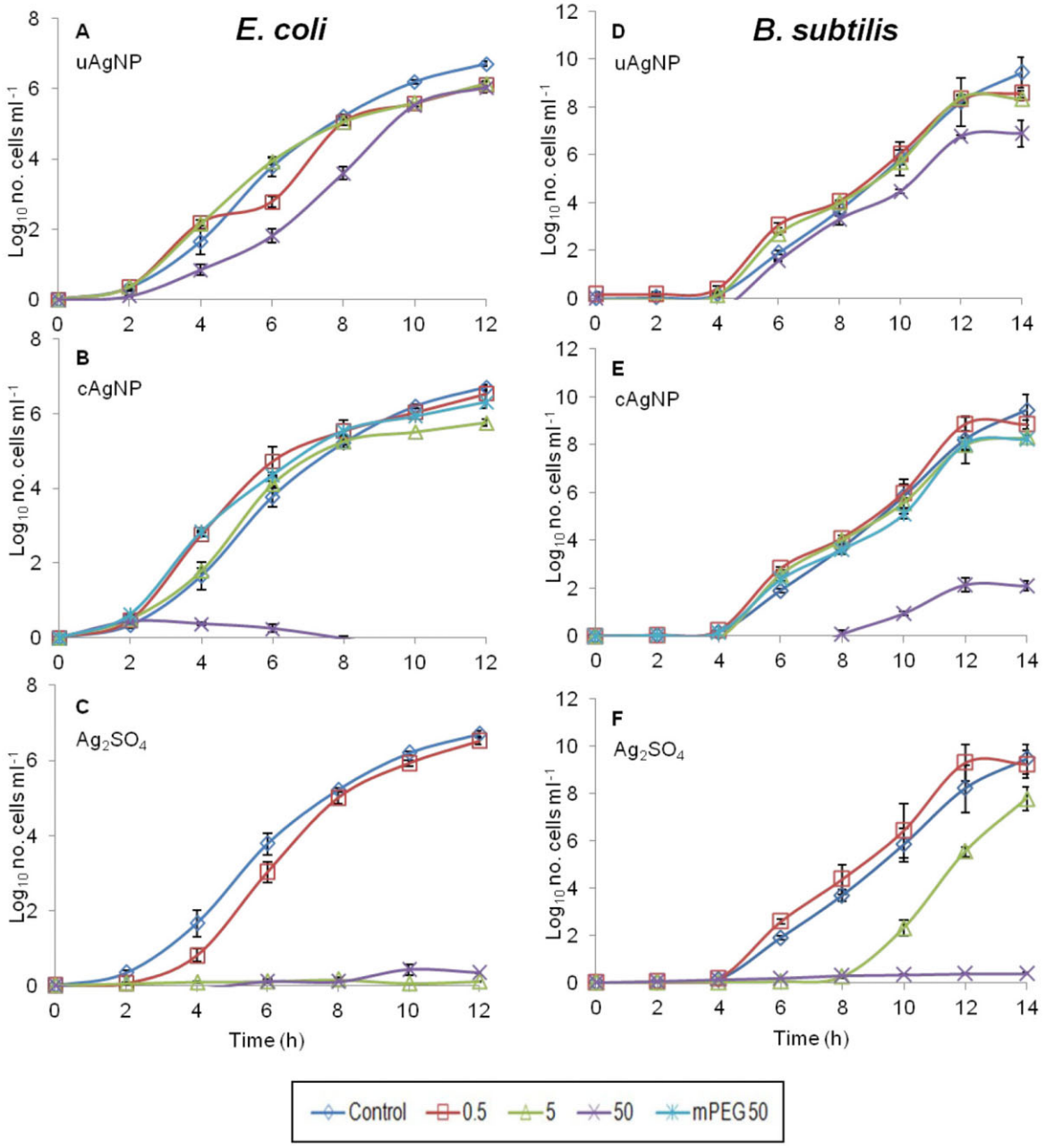

Fig. 3. Growth of *E. coli* and *B. subtilis* in the presence of uAgNPs, cAgNPs, Ag_2SO_4 (at 0.5, 5 and 50 mg l^{-1} concentrations) and mPEG at its equivalent concentration in 50 mg l^{-1} cAgNPs (111 mg l^{-1}). Error bars represent the standard error of the mean ($n = 3$).

densities were not significantly different from controls, but with 5 mg l^{-1} cAgNPs, cell densities were significantly reduced (0.6×10^6 cells ml^{-1}; $P < 0.05$) after 12 h compared with controls (5.1×10^6 cells ml^{-1}) and with 50 mg L^{-1} cAgNPs, *E. coli* cell growth was completely inhibited (Fig. 3B). Other studies have also shown that nanosilver particles are cytotoxic to *E. coli* (Pal *et al.*, 2007; Yoon *et al.*, 2007; Ruparelia *et al.*, 2008; Martinez-Gutierrez *et al.*, 2010). With 0.5 mg l^{-1} Ag_2SO_4, there was > 50% reduction to *E. coli* cell growth after 4 h until cell densities recovered to 3.2×10^6 cells ml^{-1} after 14 h, which was not significantly different from the controls (Fig. 3C). Furthermore, with 5 and 50 mg l^{-1} Ag_2SO_4, *E. coli* cell growth was completely inhibited (Fig. 3C).

With uAgNPs at 0.5 and 5 mg l^{-1}, *B. subtilis* growth was not significantly different to controls (Fig. 3D). However, with 50 mg l^{-1} uAgNP, the final cell density of *B. subtilis* after 14 h was significantly reduced (7.9×10^6 cells ml^{-1};

$P < 0.005$) (Fig. 3D). With cAgNPs at 0.5 and 5 mg l^{-1}, *B. subtilis* cell growth was not significantly affected after 14 h, but with 50 mg l^{-1} cAgNP, cell growth was significantly inhibited, resulting in an extended lag phase and a final cell density of 1.2×10^2 cells ml^{-1} after 14 h ($P < 0.001$) (Fig. 3E). With 0.5 mg l^{-1} of Ag_2SO_4, the cell density of *B. subtilis* was not significantly different to controls, but with 5 mg l^{-1} Ag_2SO_4, there was an extended lag phase of 4 h, although cell densities after 14 h (6.1×10^7 cells ml^{-1}) were not significantly reduced compared with controls (Fig. 3F). Ag_2SO_4 completely inhibited *B. subtilis* cell growth at 50 mg l^{-1} (Fig. 3F). Both *E. coli* and *B. subtilis* growth was not significantly affected by the mPEG capping agent alone, confirming that it did not contribute to the antimicrobial activity of cAgNPs (at cAgNP concentrations up to 50 mg l^{-1}) (Fig. 3B and E).

In general, *B. subtilis* showed slightly more tolerance to nanosilver than *E. coli*, especially when exposed to Ag_2SO_4. In contrast with our study, others have shown that *B. subtilis* is more susceptible to nanosilver than *E. coli* (Yoon *et al*., 2007; Ruparelia *et al*., 2008). The differences in our results and that of others may be due to different strains used that demonstrate different nanosilver tolerances. In addition, in our study, the AgNPs were suspended in liquid broth compared with being placed on disks on agar plates as in the case of Ruparelia and colleagues (2008). One possible explanation for the differential toxic effects observed between *E. coli* and *B. subtilis* is that the AgNPs may bind to the teichoic acids found in Gram-positive cell walls and are in direct competition with divalent cations that may be present in the uncharacterized components of the yeast extract and tryptone in the LB broth, thus reducing nanoparticle bioavailability. However, studies by Chudasama and colleagues (2010), and Jin and colleagues (2010) have contradictory opinions of the role of the cell wall in reducing/enhancing nanoparticle-bacterial interactions and hence toxicity.

Specifically in our study, the cAgNPs were more toxic to both *E. coli* and *B. subtilis* compared with the uAgNPs. Herein, it was notable that the cAgNPs were less likely to aggregate both in UHP water and in LB broth, whereas the uAgNPs were present as aggregates in UHP water and formed larger particles in LB broth. Increases in nanoparticle size caused by aggregation can lead to a reduction in the specific surface area (dependent on size distribution and fractal dimension of aggregate) and thus influence nanoparticle toxicity (Handy *et al*., 2008a,b; Jin *et al*., 2010; Tejamaya *et al*., 2012). It is also possible that increased aggregation and therefore settling in the uAgNPs resulted in reduced exposure and thus lower toxicity. However, throughout the experiment, the flasks were gently shaken at 150 r.p.m. to reduce sedimentation of both the bacterial cells and AgNPs. It is therefore more likely that the observed reduction in the antimicrobial potential of the uAgNPs towards *E. coli* and *B. subtilis* when grown in LB broth was due to increased aggregation and thus reduced specific surface area of the AgNPs, which either reduced AgNP: bacteria interactions or reduced AgNP dissolution rates.

It is also possible that uncharacterized components of the yeast extract and tryptone in the LB broth (such as thiol-containing amino acids) influenced nanoparticle stability (i.e. the tendency of the particles to aggregate) and bioavailability. Furthermore, the NaCl content [i.e. 1% (w/v)] of the LB broth may have led to uAgNP instability. Even small increases in salinity can affect the surface charge of AgNPs, causing them to destabilize and aggregate (Christian *et al*., 2008; Handy *et al*., 2008a). In contrast with the uAgNPs, greater colloidal stability is likely to have been provided to the cAgNPs by the mPEG capping agent (Tejamaya *et al*., 2012).

To further investigate differences in antibacterial potential of the AgNPs, the Microtox assay was performed. Ag_2SO_4 was highly toxic with an effective concentration on 50% inhibition (EC_{50}) of 1.73 mg l^{-1} (Supporting Information Table S1 and Fig. S4). Although EC_{50} values were not obtained for either uAgNPs or cAgNPs, EC_{10} values revealed 20% greater toxic response elicited by the cAgNPs (EC_{10} 32 mg l^{-1}) compared with uAgNPs (EC_{10} 40 mg l^{-1}). It is possible that the uAgNPs aggregated in the high ionic strength [2% (w/v)] Microtox diluent, which may have reduced its overall toxicity and would explain the differential toxicities observed between the cAgNPs and uAgNPs. Because the mPEG alone did not elicit a toxic response (at its equivalent concentration in up to 450 mg l^{-1} cAgNPs), it was assumed that the capping agent did not exacerbate the toxicity of the cAgNPs to *Vibrio fischeri* (Supporting Information Table S1 and Fig. S4).

Interactions between E. coli*, AgNPs and* Ag_2SO_4

To enhance our understanding of bacterial responses to specific AgNPs and hence possible causes of cellular toxicity, *E. coli* cells were incubated with uAgNPs, cAgNPs and Ag_2SO_4, and scanning TEM (STEM) performed to identify specific AgNP-bacterial interactions (Fig. 4). When *E. coli* cells were incubated with 50 mg l^{-1} Ag_2SO_4, there was a 45% increase in the number of damaged cells (either partially or completely) compared with controls. With cAgNPs, there was a 39% increase, and with uAgNPs, there was a 33% increase in the number of damaged cells (compared with controls). In some cases, where specific areas of cell membrane had been damaged (Fig. 4A, indicated by black arrows), *E. coli* cell contents were released into the surrounding environment. Energy dispersive X-ray (EDX) spectros-

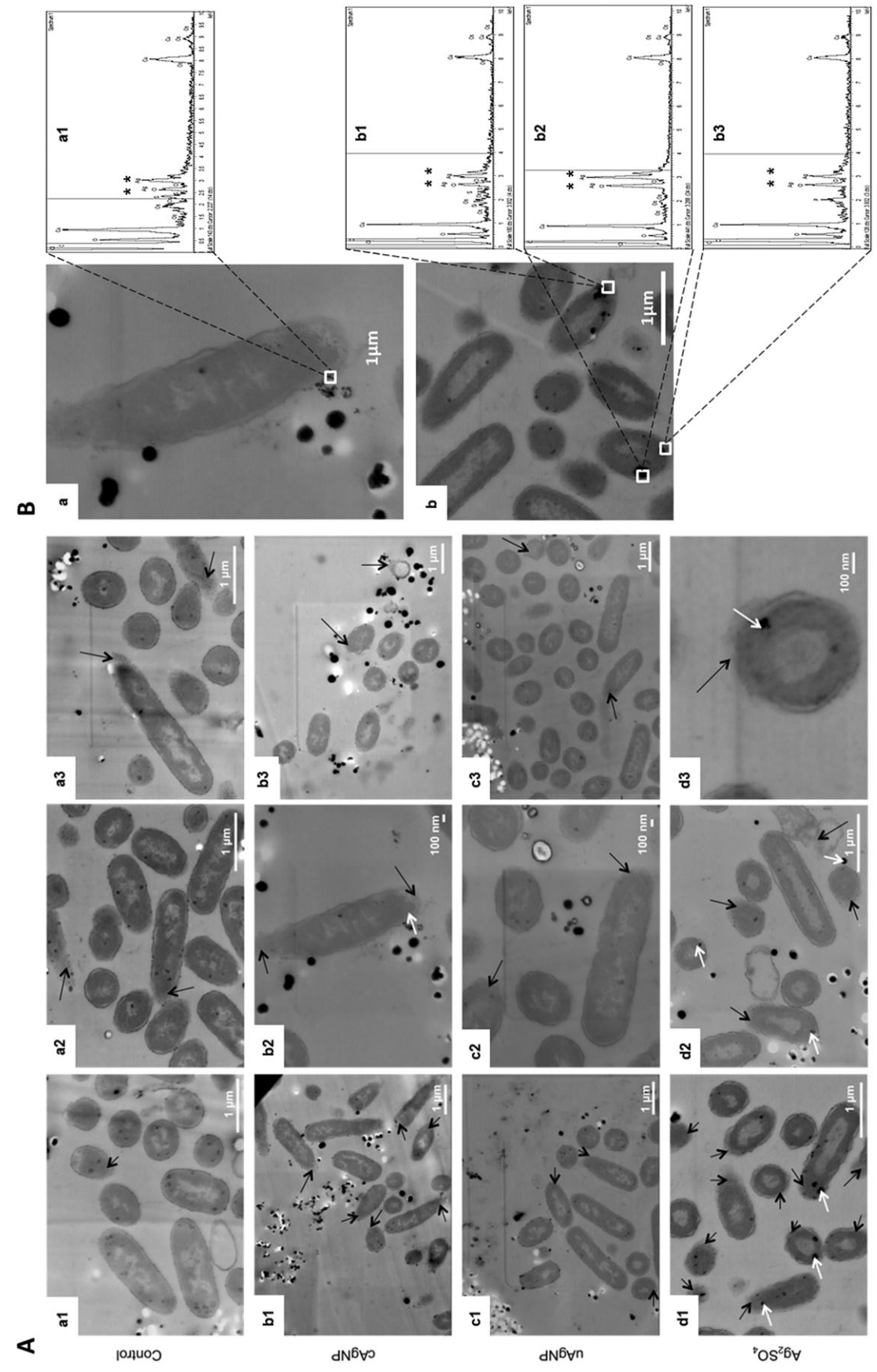

Fig. 4. Representative STEM micrographs showing untreated *E. coli* cells (a1–3) and *E. coli* cells exposed to 50 mg l^{-1} cAgNPs (b1–3), uAgNPs (c1–3) and Ag_2SO_4 (d1–3). Black arrows indicate areas of cell wall damage and white arrows indicate areas where Ag was detected by EDX (A); representative STEM micrographs showing the effect of AgNPs on *E. coli* cells exposed to 50 mg l^{-1} cAgNPs (a) and 50 mg L^{-1} Ag_2SO_4 (b). White boxes indicate areas where Ag was detected by EDX, and corresponding EDX spectrum are shown (a1, b1–3) with Ag peaks marked (*) (B).

copy was applied to determine the specific location of Ag in and around *E. coli* cells, and although Ag was not directly detected within *E. coli* cells when incubated with uAgNPs, it was detected close to areas of damaged cell membranes in samples incubated with cAgNPs, and inside cell cytoplasm and around cell membranes with cultures incubated with Ag_2SO_4 (Fig. 4B, indicated by white arrows).

It is well known that AgNPs exhibit size-dependent toxicity, which may be due to either a direct effect of increased contact between the surface of the smaller particles and cell membranes (Sondi and Salopek-Sondi, 2004), or an indirect effect caused by increased dissolution of Ag^+ from smaller AgNPs compared with larger AgNPs (Sotiriou *et al*., 2011; Ma *et al*., 2012; Xiu *et al*., 2012). It has been suggested that AgNPs may attach to and penetrate bacterial cell membranes (Sondi and Salopek-Sondi, 2004). Physical damage to cell membranes leading to increased membrane permeability, loss of membrane transport control and ultimately, cell death has been suggested as one of the primary causes of AgNP toxicity (Sondi and Salopek-Sondi, 2004; El Badawy *et al*., 2011). In the present study, increased bacterial cell membrane damage was observed in the presence of AgNPs and Ag_2SO_4. Furthermore, Ag was detected by EDX near to areas of *E. coli* cell membrane damage following incubation with cAgNPs, indicating a direct role for cAgNPs in bacterial cell membrane damage.

It is possible that an indirect effect of size-dependent AgNP toxicity was caused by increased dissolution of Ag^+ from the smaller AgNPs. However, we have shown that there was no difference in the rate of Ag^+ dissolution between the cAgNPs and the uAgNPs measured over 51 h (i.e. encompassing the time the model bacteria were exposed to AgNPs) (Supporting Information Fig. S3). Thus, size differences between cAgNPs and uAgNPs (including specific surface area and aggregation behaviour) rather than Ag^+ dissolution are thought to have contributed to the observed differences in antibacterial activities herein. It is possible, however, that greater Ag^+ dissolution from AgNPs may occur over longer periods of time (Kittler *et al*., 2010), which may have severe long-term implications to *in situ* environmental microbial communities and their processes. In the present study, Ag_2SO_4 (as a source of dissolved silver) had the greatest inhibitory effect on all of the bacteria tested. Ag^+ dissolution from Ag_2SO_4 was greater than that observed for the AgNPs over 51 h (Supporting Information Fig. S3) and may account for the observed increase in toxicity compared with AgNPs. Several previous studies have also demonstrated that dissolved silver (usually in the form of $AgNO_3$) is more toxic than AgNPs to bacteria (Choi *et al*., 2008; Jin *et al*., 2010; Pokhrel *et al*., 2012).

In conclusion, the inhibitory effect of the different Ag species was in the following order Ag_2SO_4 > cAgNP > uAgNP. It was notable that the cAgNPs had a greater inhibitory effect on AOB NPRs compared with uAgNPs. Generally, *Nitrosomonas europaea* demonstrated greater sensitivity to AgNPs (even at lower concentrations). Although the drivers for the observed differences in inhibition by the nanoparticles to the bacteria are not entirely clear, it is likely that size differences (rather than the capping agent itself) may have played a role (i.e. the cAgNPs were up to fivefold smaller than the uAgNPs). Our findings demonstrate that in systems such as wastewater treatment plants where nitrification-denitrifcation processes are important for nitrate removal, the accumulation of AgNPs is likely to have a detrimental effect on AOB activities (especially *Nitrosomonas europaea*), which may lead to system failures. Furthermore, following the release of AgNPs into receiving environments, the activities of AOB and faecal indicator organisms such as *E. coli* will be severely impacted. In nanoparticle studies, it is also important to investigate the effect of weathering processes on engineered nanoparticles (ENPs) and its effect on microorganisms, as exposure of organisms in the environment to ENP will occur not only via wastewater from manufacturers but also via municipal wastewater and direct inputs from weathering and ageing of products containing nanomaterials. It is therefore important that studies such as this focus on the impact of ENP on ecologically important groups of microorganisms like AOB.

Acknowledgements

This work was supported by a Natural Environment Research Council (NERC) CASE studentship with CEFAS (Ref: NE/H525289/1) and the University of Essex. The support of the NERC Facility for Environmental Nanoscience Analysis and Characterization is acknowledged. We thank Mr. Farid Benyahia for technical assistance and Dr. Terry McGenity for useful comments on the manuscript.

References

Baalousha, M., and Lead, J.R. (2012) Rationalizing nanomaterial sizes measured by atomic force microscopy, flow field-flow fractionation and dynamic light scattering: sample preparation, polydispersity and particle structure. *Environ Sci Technol* **46:** 6134–6142.

Bedard, C., and Knowles, R. (1989) Physiology, biochemistry and specific inhibitors of CH_4, NH_4^+, and CO oxidation by methanotrophs and nitrifiers. *Microbiol Rev* **53:** 68–84.

Choi, O., Deng, K., Kim, N., Ross, L., Surampalli, R., and Hu, Z. (2008) The inhibitory effects of silver nanoparticles, silver ions and silver chloride colloids on microbial growth. *Water Res* **42:** 3066–3074.

Christian, P., von der Kammer, F., Baalousha, M., and Hofmann, T. (2008) Nanoparticles: structure, properties,

preparation and behaviour in environmental media. *Ecotoxicology* **17:** 326–343.
Chudasama, B., Vala, A.K., Andhariya, N., Mehta, R.V., and Upadhyay, R.V. (2010) Highly bacterial resistant silver nanoparticles: synthesis and antibacterial activities. *J Nanopart Res* **12**: 1677–1685.
Domingos, R.F., Baalousha, M.A., Ju-Nam, Y., Reid, M.M., Tufenkji, N., Lead, J.R., *et al*. (2009) Characterizing manufactured nanoparticles in the environment: multimethod determination of particle sizes. *Environ Sci Technol* **43:** 7277–7284.
El Badawy, A.M., Silva, R.G., Morris, B., Scheckel, K.G., Suidan, M.T., and Tolaymat, T.M. (2011) Surface charge-dependent toxicity of silver nanoparticles. *Environ Sci Technol* **45:** 283–287.
Gottschalk, F., Sonderer, T., Scholz, R.W., and Nowack, B. (2009) Modeled environmental concentrations of engineered nanomaterials (TiO_2, ZnO, Ag, CNT, Fullerenes) for different regions. *Environ Sci Technol* **43:** 9216–9222.
Handy, R., Owen, R., and Valsami-Jones, E. (2008a) The ecotoxicology of nanoparticles and nanomaterials: current status, knowledge gaps, challenges, and future needs. *Ecotoxicology* **17:** 315–325.
Handy, R., von der Kammer, F., Lead, J., Hassellöv, M., Owen, R., and Crane, M. (2008b) The ecotoxicology and chemistry of manufactured nanoparticles. *Ecotoxicology* **17:** 287–314.
Jin, X., Li, M., Wang, J., Marambio-Jones, C., Peng, F., Huang, X., *et al*. (2010) High-throughput screening of silver nanoparticle stability and bacterial inactivation in aquatic media: influence of specific ions. *Environ Sci Technol* 2010, **44:** 7321–7328.
Joye, S.B., and Hollibaugh, J.T. (1995) Influence of sulfide inhibition of nitrification on nitrogen regeneration in sediments. *Science* **270:** 623–625.
Kim, J.S., Kuk, E., Yu, K.N., Kim, J., Park, S.J., Lee, H.L., *et al*. (2007) Antimicrobial effects of silver nanoparticles. *Nanomedicine* **3:** 95–101.
Kittler, S., Greulich, C., Diendorf, J., Köller, M., and Epple, M. (2010) Toxicity of silver nanoparticles increases during storage because of slow dissolution under release of silver ions. *Chem Mater* **22:** 4548–4554.
Klaine, S., Alvarez, P., Batley, G., Fernandes, T., Handy, R., Lyon, D., *et al*. (2008) Nanomaterials in the environment: behavior, fate, bioavailability, and effects. *Environ Toxicol Chem* **27:** 1825–1851.
Kowalchuck, G.A., and Stephen, J.R. (2001) Ammonia-oxidising baceria: a model for molecular microbial ecology. *Annu Rev Microbiol* **55:** 485–529.
Ma, R., Levard, C., Marinkos, S., Cheng, Y., Liu, J., Michel, F.M., *et al*. (2012) Size-controlled dissolution of organic-coated silver nanoparticles. *Environ Sci Technol* **46:** 752–759.
MacCuspie, R.I., Rogers, K., Patra, M., Suo, Z., Allen, A.J., Martin, M.N., and Hackley, V.A. (2011) Challenges for physical characterization of silver nanoparticles under pristine and environmentally relevant conditions. *J Environ Monit* **13:** 1212–1226.
Martinez-Gutierrez, F., Olive, P.L., Banuelos, A., Orrantia, E., Nino, N., Sanchez, E.L., *et al*. (2010) Synthesis, characterisation, and evaluation of antimicrobial and cytotoxic effect of silver and titanium nanoparticles. *Nanomedicine* **6:** 681–688.
Moore, M. (2006) Do nanoparticles present ecotoxicological risks for the health of the aquatic environment? *Environ Int* **32:** 967–976.
Nicol, G.W., Leininger, S., Schleper, C., and Prosser, J.I. (2008) The influence of soil pH on the diversity, abundance and transcriptional activity of ammonia oxidising archaea and bacteria. *Environ Microbiol* **10:** 2966–2978.
Nowack, B., and Bucheli, T. (2007) Occurrence, behavior and effects of nanoparticles in the environment. *Environ Pollut* **150:** 5–22.
Pal, S., Tak, Y.K., and Song, J.M. (2007) Does the antibacterial activity of silver nanoparticles depend on the shape of the nanoparticles? A study of the gram-negative bacterium Escherichia coli. *Appl Environ Microbiol* **73:** 1712–1720.
PEN (2013) *The Woodrow Wilson International Center for Scholars*, Project on Emerging Nanotechnologies website [WWW document]. URL http://www.nanotechproject.org.
Pokhrel, L.R., Silva, T., Dubey, B., Badawy, A.M., Tolaymat, T.M., and Scheuerman, P.R. (2012) Rapid screening of aquatic toxicity of several metal-based nanoparticles using the MetPlate™ bioassay. *Sci Total Environ* **426:** 414–422.
Prosser, J.I. (1989) Autotrophic nitrification in bacteria. *Adv Microb Physiol* **30:** 125–181.
Prosser, J.I., and Nicol, G.W. (2008) Relative contributions of archaea and bacteria to aerobic ammonia oxidation in the environment. *Environ Microbiol* **10:** 2931–2941.
Ruparelia, J.P., Chatterjee, A.K., Duttagupta, S.P., and Mukherji, S. (2008) Strain specificity in antimicrobial activity of silver and copper nanoparticles. *Acta Biomater* **4:** 707–716.
Rysgaard, S., Thastum, P., Dalsgaard, T., Christensen, P.B., and Sloth, N.P. (1999) Effect of salinity on NH_4 adsorption capacity, nitrification, and denitrification in Danish estuarine sediments. *Estuaries* **22**: 21–30.
Siripong, S., and Rittmann, B.E. (2007) Diversity of nitrifying bacteria in full-scale municipal wastewater treatment plants. *Water Res* **41:** 1110–1120.
Sondi, I., and Salopek-Sondi, B. (2004) Silver nanoparticles as antimicrobial agent: a case study on *E. coli* as a model for Gram-negative bacteria. *J Colloid Interface Sci* **275:** 177–182.
Sotiriou, G.A., Teleki, A., Camenzind, A., Krumeich, F., Meyer, A., Panke, S., and Pratsinis, S.E. (2011) Nanosilver on nanostructured silica: antibacterial activity and Ag surface area. *Chem Eng J* **170:** 547–554.
Strauss, E.A., and Dodds, W.K. (1997) Influence of protozoa and nutrient availability on nitrification rates in subsurface sediments. *Microb Ecol* **34:** 155–165.
Tejamaya, M., Römer, I., Merrifield, R.C., and Lead, J. (2012) Stability of citrate, PVP and PEG coated silver nanoparticles in ecotoxicology media. *Environ Sci Technol* **46:** 7011–7017.
Xiu, Z., Zhang, Q., Puppala, H.L., Colvin, V.L., and Alvarez, P.J.J. (2012) Negligible particle-specific antibacterial activity of silver nanoparticles. *Nano Lett* **12:** 4271–4275.
Yoon, K.-Y., Byeon, J.H., Park, J.-H., and Hwang, J. (2007) Susceptibility contants of *Escherichia coli* and *Bacillus*

subtilis to silver and copper nanoparticles. *Sci Total Environ* **373:** 572–575.

Supporting information

Additional Supporting Information may be found in the online version of this article at the publisher's web-site:

Fig. S1. Representative AFM micrographs of cAgNPs.
Fig. S2. Nanoparticle hydrodynamic diameter distributions determined by FlFFF.
Fig. S3. Dissolution of Ag+ from AGNPs and Ag_2SO_4 in UHP water over 51 h. uAgNPs (closed squares), cAgNPs (closed diamonds) and Ag_2SO_4 (closed triangles).
Fig. S4. Microtox® assay for AgNPs, mPEG and Ag_2SO_4. Dotted lines depicting effective concentrations (ECs) at 10%, 20% and 50% inhibition are shown. Error bars represent the standard error of the mean ($n = 3$).
Fig. S5. Z-average diameter of uAgNPs for 4 days following different lengths of sonication time. Error bars represent the standard error of the mean ($n = 15$).
Table S1. Effective concentrations (ECs) in mg l^{-1} for 10%, 20% and 50% inhibition by uAgNPs, cAgNPs, mPEG and Ag_2SO_4 measured by Microtox®. Shaded boxes represent hypothetical values based on linear equations from Supporting Information Fig. S2.
Appendix S1. Experimental procedures.